

THE PENNSYLVANIA STATE UNIVERSITY
COLLEGE OF EARTH AND MINERAL SCIENCES

DEPARTMENT OF GEOSCIENCES

Numerical Modelling of Lake Bonneville Paleoshoreline Erosion at Mars-Like Rates and Durations

A Thesis in Geosciences

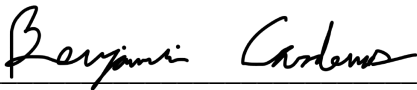
by

Zachary J. Baran

Submitted in partial fulfillment
of the requirements
for the degree of

Bachelor of Science
Fall 2023

Reviewed and approved by:



Advisor's Name, Professor of Geosciences

December 12, 2023

Date

Charles J. Ammon, Professor of Geosciences
Associate Head for Undergraduate Programs

Date

Abstract

Mars is currently very cold and arid, with conditions that do not permit liquid water. However, this may not always have been the case. Earlier in Mars' history, atmospheric conditions may have not only permitted water, but there may have been enough for an ocean-like body of water to exist in the planet's northern hemisphere until around 3.5 Gya. One interpretation used to support the existence of this ocean has been laterally extensive paleoshoreline features, originally interpreted via textural differences. They remain contentious and deserve skepticism. Uncontentious paleoshorelines exist on Earth and are recognized not by textural differences, but rather topography. Their determinant feature is subtle breaks in hillslope with locally high slopes. The purpose of this experiment is to investigate whether these features would have even been able to survive 3.5 Ga of slow Martian erosion. Despite the erosive forces on Mars being slow, given the long timescale of which these paleoshoreline features would have had to endure exposure to them, preservation seems unlikely. To investigate this, I obtained topographic data containing known terrestrial paleoshorelines in Utah, originating from Pleistocene paleolake Bonneville, and ran a numerical linear hillslope diffusion model on this topography at Mars-like rates and durations.

Table of Contents

Acknowledgements..... 4
Introduction..... 5
Lake Bonneville Background..... 12
Methods..... 12
Results..... 18
Discussion..... 22
Conclusion..... 23
References Cited 24

Acknowledgments

I would like to thank my advisor, Benjamin Cardenas, for his guidance, as well as all the Planetary Sedimentology Lab group members for their support and feedback throughout the research and writing process. Additionally, I would like to thank my friends and family for their continued support and for letting me ramble on about Mars and rocks.

Introduction

Present day Mars is very cold and arid, with surface conditions that do not permit liquid water (Carr and Head III, 2010). This cold, dry Mars has existed for the past three billion years, during the planet's Amazonian period, of which it is still in today (Figure 1).

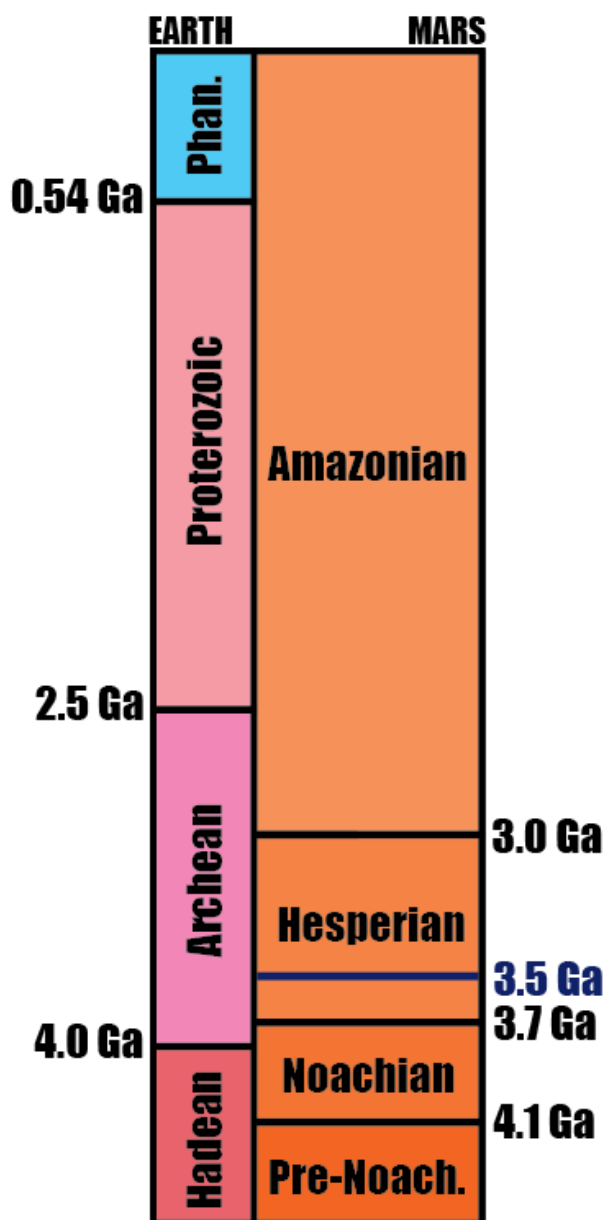


Figure 1. Comparative geologic timescale showing both Earth's (left) and Mars' (right). Based on timescale from Carr and Head III, 2003. Blue marker at 3.5 Ga represents time that the proposed ocean would have ceased to be present in the Northern hemisphere

However, during earlier geologic periods, conditions were more conducive to an active hydrologic cycle. There is abundant evidence that water flowed in rivers that both carved land, incising the deep and integrated valley networks (Howard et al., 2005; Carr and Head III, 2010; Costard et al., 2017; Carr and Head, 2019), and rivers that net-deposited sediment, building up stratigraphy over time (Grotzinger et al., 2015). The ancient climate may have even permitted an ocean-like body of water (Carr and Head, 2019). Mars has a unique dichotomous global morphology, of which the northern hemisphere is characterized by a relatively smooth surface that is lower in elevation than the higher elevation, more cratered southern hemisphere (Watters et al., 2007). Several geomorphologic observations along the margin of this northern basin have been proposed as evidence to substantiate the existence of an ocean in the basin until around 3.5 Ga. Furthermore, stratigraphic interpretations of deltaic deposits near the dichotomy boundary also suggest the presence of water in the past and the potential for an ocean (DiBiase et al., 2013; Hughes et al., 2019).

Paleoshoreline interpretations along the elevation dichotomy directly support the idea of an ancient martian ocean, as they would have been formed by wave action in a basin-spanning water body. Initial interpretations of these features were based solely on imagery of the surface showing textural differences near the elevation dichotomy (Figure 2) (Parker et al., 1989; Parker et al., 1993; Maling and Edgett, 1999). These proposed paleoshorelines run very long lateral distances (~100 km in terms of order of magnitude) across the landscape, lending some credence to the hypothesis that they had been formed by a planet-spanning process. Additionally, several possible paleoshorelines have been mapped (Fig. 3) and have been used to infer water-level fluctuations over time (Sholes et al., 2021).

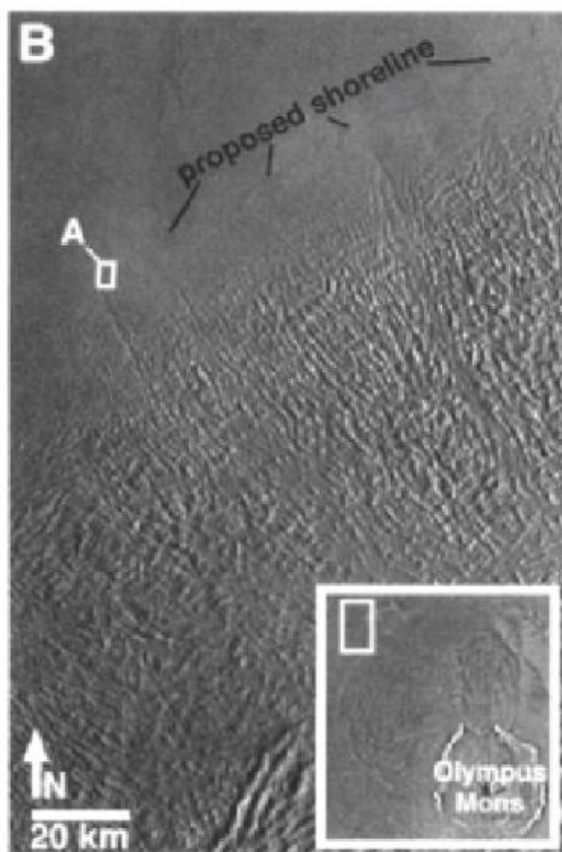
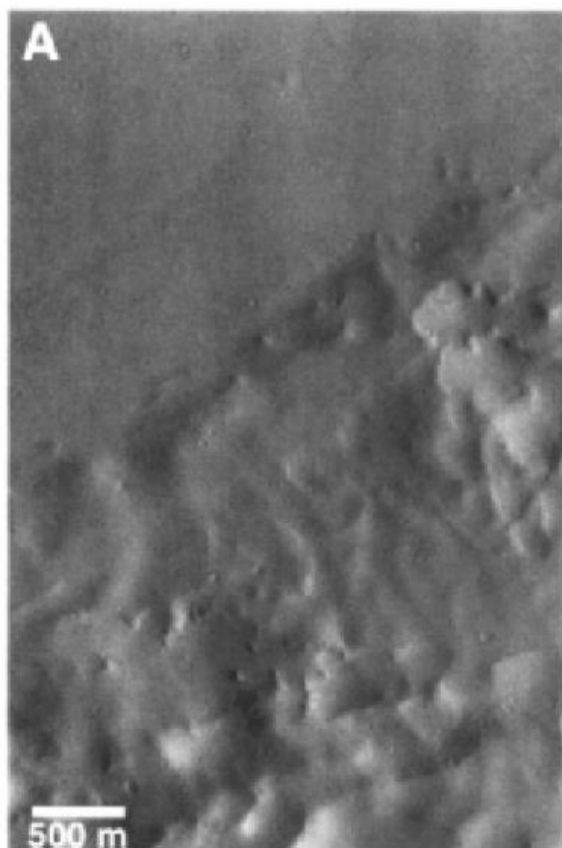


Figure 2. From Malin and Edgett, 1999. Panels a and b show textural differences along the martian elevation dichotomy that were used by Parker et al., 1989 and Parker et al., 1993 to interpret paleoshorelines. These images are higher resolution than those used in those early interpretations and are amongst the first to be used in reexamining those features.

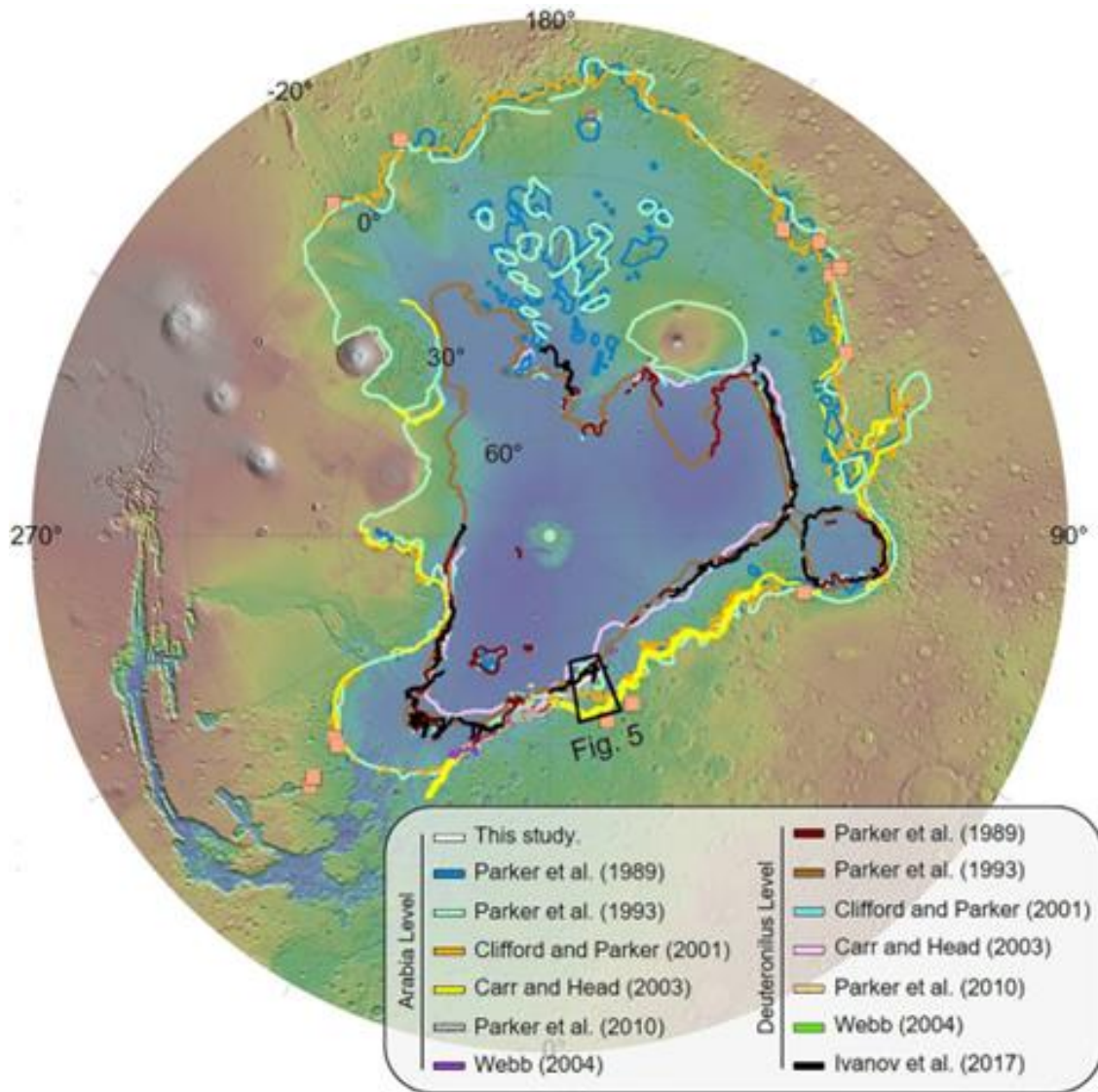


Figure 3. From Sholes et al., 2021. Map of all currently published paleoshoreline interpretations on Mars.

Despite numerous new interpretations of paleoshorelines being published in the decades since the initial interpretations (Figure 3), they remain contentious. With advancements in imaging, features previously attributed to paleoshorelines were able to be reexamined. From this, some of these features were then reattributed to volcanic contacts (Carr and Head, 2003). Reexaminations when planet-wide topographic datasets became available also revealed drastic variations in elevation, on the order of several kilometers, across the lateral extent of these features (Head III et al., 1998; Carr and Head III, 2003; Sholes et al., 2021). This is not characteristic of shorelines, as sea level follows the equal gravitational potential (Carr and Head III, 2003). Attempts have been made to explain this by attributing these elevation differences to true polar wander (Perron et al., 2007). This mechanism, which is the reorientation of the planet relative to its rotation pole, can cause long-wavelength crustal deformation over very large timescales. However, the validity of the true polar wander models has also been questioned so there is no consensus regarding the elevation differences (Sholes et al., 2021).

The main point of contention regarding the Mars paleoshoreline interpretations that most directly relates to this research, is that early interpretations were largely determined via textural differences (Parker et al., 1989; Parker et al., 1993). True determinant features used to interpret paleoshorelines on Earth are that of small-scale topography represented by subtle breaks in slope (Figure 4) — not textural differences seen in plan-view imagery (Dickinson, 2001; Hare et al., 2001).

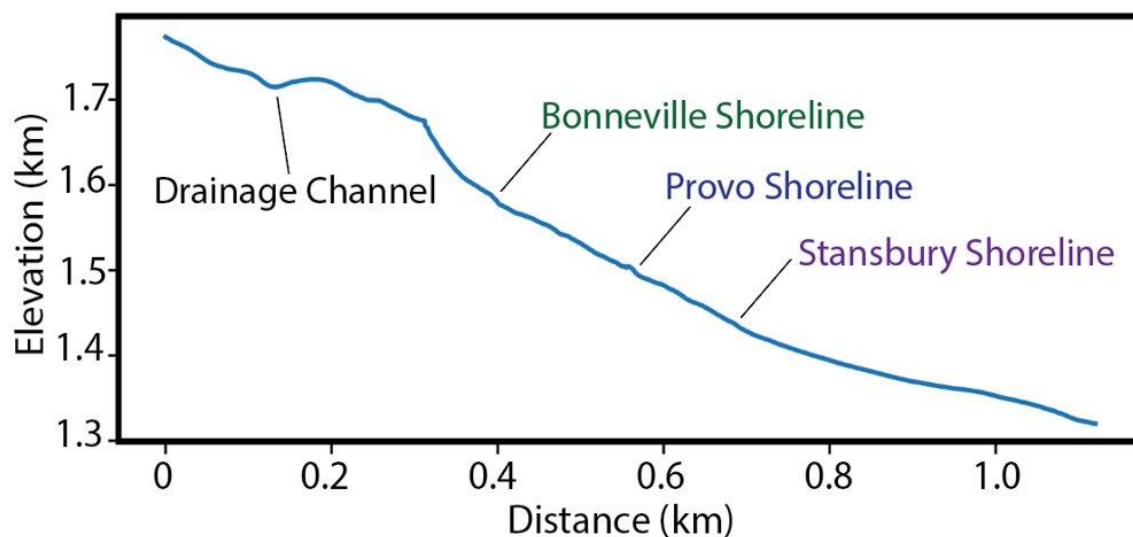


Figure 4. Profile of initial topography taken at black line ($y = 1.0$ km) seen in Figure 7. Each shoreline is denoted by a very subtle topographic break in slope. The left side of the profile is taken up by the hilly region of the DEM and the associated drainage channel present.

Is it probable, or even possible, that paleoshoreline topography on Mars might persist for 3.5 billion years, even at the slow erosion rates estimated for the martian surface? We cannot directly measure these hypothesized paleoshorelines as they were 3.5 Ga to know how they evolved, but we can use earth analogs and experiments to guide our interpretations of Mars. Here, we used topographic data showing well-preserved Earth-analog paleoshorelines, and numerically modeled their erosion at Mars-like rates and durations. Uncontested paleoshorelines exist across Earth and may be able to serve as Mars paleoshoreline analogs. Three well documented paleoshorelines with clear topographic signatures exist in modern day Utah, belonging to paleolake Bonneville (Figure 5) (Benson et al., 2011; Oviatt, 2015). We hypothesize that subtle paleoshoreline topographic features would not have been able to survive long-scale martian erosion.

Lake Bonneville Background

Pleistocene paleolake Lake Bonneville (Figure 5) existed from 30 kya to 13 kya. Across this timespan, the lake experienced several major water-level changing events that formed the three paleoshorelines (Benson et al., 2011; Oviatt, 2015). In the order of oldest to youngest they are called the Stansbury, Bonneville, and Provo shorelines. The determinant feature of paleoshoreline topography is a break in hillslope, with the slope locally transitioning from shallow above the paleo-water level to steep beneath it. They are typically formed via wave action reworking and eroding the land, which can then remain as those small topographic features following changes in water level (Dickinson, 2001; Hare et al., 2001).

Stansbury is the oldest of the three shorelines, dated at 25 ka and was formed during water level oscillations at that time. The basin continued to fill with water and eventually reached its peak height around 18 kya, represented by the Bonneville shoreline. The Bonneville flood was an event that drained water from the basin en masse because of overflowing, and it left behind the Bonneville paleoshoreline in its wake. Overflowing and flooding continued until 15 kya and the Provo paleoshoreline was created during this 18 kya – 15 kya interval (Benson et al., 2011; Oviatt, 2015).

Methods

To investigate the likelihood of Mars paleoshoreline preservation, a linear diffusivity model was run on Lake Bonneville paleoshoreline topography at Mars-like rates and durations. Northern Central Utah 2020 LiDAR, 1 meter resolution digital elevation models (DEMs) from near Promontory Point along Bear River Bay were obtained from the Utah Geospatial Research Center to create a 2.411 km by 1.121 km rectangular extent containing sections of the three

paleoshorelines (Figures 6 and 7). Names of the specific files used to compile into a larger DEM are listed in Table 1. This topographic data served as the initial topography in the model. The DEMs were converted into an array of the same dimensions for use within Python.



Figure 6. The extent of DEM used in the model (grey box) with the three paleoshorelines traced (Bonneville in green, Provo in blue, and Stansbury in purple).

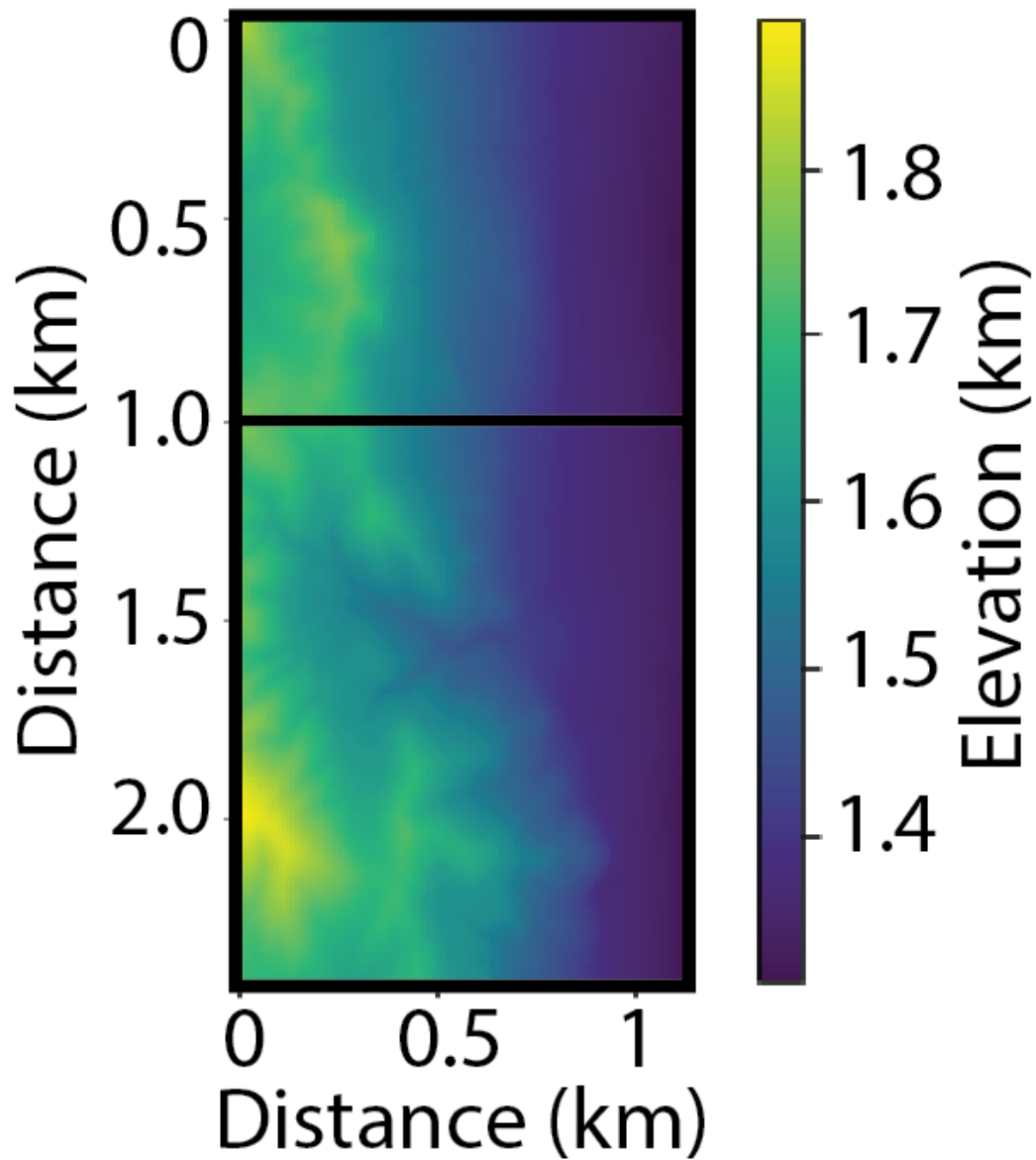


Figure 7. Initial DEM used in the experiment with the x and y axes being distance and the color bar showing the elevation. The black bar at $y = 1.0$ km is where transects were taken to view shoreline topography in profile view (Figures 9).

DEM File Names
12TUL8370
12TUL8270
12TUL8269
12TUL8268
12TUL8266
12TUL8171
12TUL8170
12TUL8169
12TUL8168
12TUL8167
12TUL8166
12TUL8071
12TUL8070
12TUL8069
12TUL8068
12TUL8067
12TUL7967
12TUL8370

Table 1. File Names from the Utah Geospatial Research website.

A linear hillslope diffusion model was created using the LandLab module for Python (Hobley et al., 2017; Barnhart et al., 2020; Hutton et al., 2020). The governing equation behind the model is as follows:

$$\frac{dz}{dt} = D \times \nabla \quad (\text{Eq. 1})$$

Here, $\frac{dz}{dt}$ is the change in elevation over time (m yr^{-1}), D is the diffusion coefficient (or simply diffusivity, m^2yr^{-1}), and ∇ is the curvature of the hillslope (m^{-1}) (Martin, 2000). Several erosional mechanisms act on Mars' surface, but they are generally slower than those on Earth (Diniega et al., 2021). Some of these mechanisms, like soil creep or micro-impacting, behave diffusively and are classified as hillslope processes (Howard, 2007). Diffusive hillslope processes can be modelled mathematically via linear hillslope diffusion.

Diffusivity values, D , have been measured across Earth and are a function of climate and lithology (Richardson et al., 2019). Due to this, the range of diffusivities observed on Earth varies by several magnitudes. The Atacama Desert has a measured diffusivity value amongst the lowest on Earth, at $10^{-4} \text{ m}^2\text{yr}^{-1}$ (Richardson et al., 2019). Mars diffusivities have been estimated by observing the crustal erosion at impact craters, and they range from $10^{-9} \text{ m}^2\text{yr}^{-1}$ to $10^{-5} \text{ m}^2\text{yr}^{-1}$ (Howard 2007; Golombek et al., 2014; Kite and Mayer, 2017).

We performed twelve experiments, during which two variables were changed and one was kept constant. One of the variables we varied across experiments was the diffusivity value, D (Eq. 1). Three values were chosen to represent Mars like conditions: $10^{-9} \text{ m}^2\text{yr}^{-1}$, $10^{-7} \text{ m}^2\text{yr}^{-1}$ and $10^{-5} \text{ m}^2\text{yr}^{-1}$ (Howard 2007; Golombek et al., 2014). The Atacama Desert diffusivity, 10^{-4}

$4m^2yr^{-1}$, was also used in the model to compare how shoreline features fare against Earth erosional values (Richardson et al., 2019).

The second variable that was altered throughout the experiments was a scale multiplier. The x and y dimensions of the landscape were represented by the dimensions of the array, and the elevation data (z axes) was stored within the array. Multiplier values of 1, 10, or 100, were applied to the three dimensions, keeping the overall geometry of the topography the same while increasing its size, in terms of area and relief, across experiments. Experiments with multiplier values of 1 were the same $2.411 \text{ km} \times 1.121 \text{ km}$ as the original DEM boundary, whereas for multipliers of 10 and 100, these increased to $24.11 \text{ km} \times 11.21 \text{ km}$ and $241.1 \times 112.1 \text{ km}$ respectively. Total initial relief for the multiplier 1 experiments was also the same as the original DEM at $\sim 0.6 \text{ km}$, and for multiplier 10 and 100 experiments, initial relief was $\sim 6 \text{ km}$ and $\sim 60 \text{ km}$ respectively. This was to test how the scale of shoreline features affects their preservation, with the assumption that $10\times$ and $100\times$ features will erode slower than those at $1\times$ scale. Time was kept constant for each experiment, with 3.5 billion years being simulated across 350, 10^6 year timesteps. These experimental parameter combinations are displayed in Table 2.

Table 2. Variables Across Experiments

EXPERIMENT	1	2	3	4	5	6	7	8	9	10	11	12
TIME (GA)	3.5	3.5	3.5	3.5	3.5	3.5	3.5	3.5	3.5	3.5	3.5	3.5
DIFFUSIVITY (M²YR⁻¹)	10^{-4}	10^{-5}	10^{-7}	10^{-9}	10^{-4}	10^{-5}	10^{-7}	10^{-9}	10^{-4}	10^{-5}	10^{-7}	10^{-9}
MULTIPLIER	1	1	1	1	10	10	10	10	100	100	100	100

A DEM and slope map was saved at every timestep for all twelve experiments. Topographic difference maps were created by subtracting the data in the initial DEMs from the timestep 350 (final) DEMs. Transects were made from each DEM along the line $y = 1 \text{ km} \times \text{multiplier value}$ ($y = 1 \text{ km}$, 10 km , or 100 km). Shoreline preservation was determined visually by examining these transects throughout time.

Results

Figure 8 shows an array of difference maps produced from each of the twelve experiments. The columns represent which diffusivity was used, and the rows represent the scale. The stair-step dividing line separates experiments that showed little topographic change from those that showed visible erosion. On the left side of the line, the maps appear nearly monochromatic. This monochromatic teal is associated with very little change in the topography in any of these six experiments. On the right side of the line, the difference maps show more variability in color, meaning that the model noticeably eroded the landscape. Shades of yellow represent a positive change associated with sediment infilling, and shades of blue and purple represent erosion. In particular, the difference maps show that the most change occurred at locations that match the positions of the modern-day paleoshorelines, as well as the drainage network that postdates and cross-cuts the paleoshorelines. This should be expected, given that these are the regions with the steepest initial slopes, and diffusive erosion will most rapidly rework steep slopes. The most drastic topographic changes occurred in experiments using $1 \times$ multipliers and high diffusivities ($10^{-5} \text{ m}^2 \text{ yr}^{-1}$ and $10^{-4} \text{ m}^2 \text{ yr}^{-1}$). Experiments at $10 \times$ and $100 \times$

scale, and those at low diffusivities ($10^{-7} \text{ m}^2 \text{ yr}^{-1}$ and $10^{-9} \text{ m}^2 \text{ yr}^{-1}$), showed no noticeable topographic change in the difference maps.

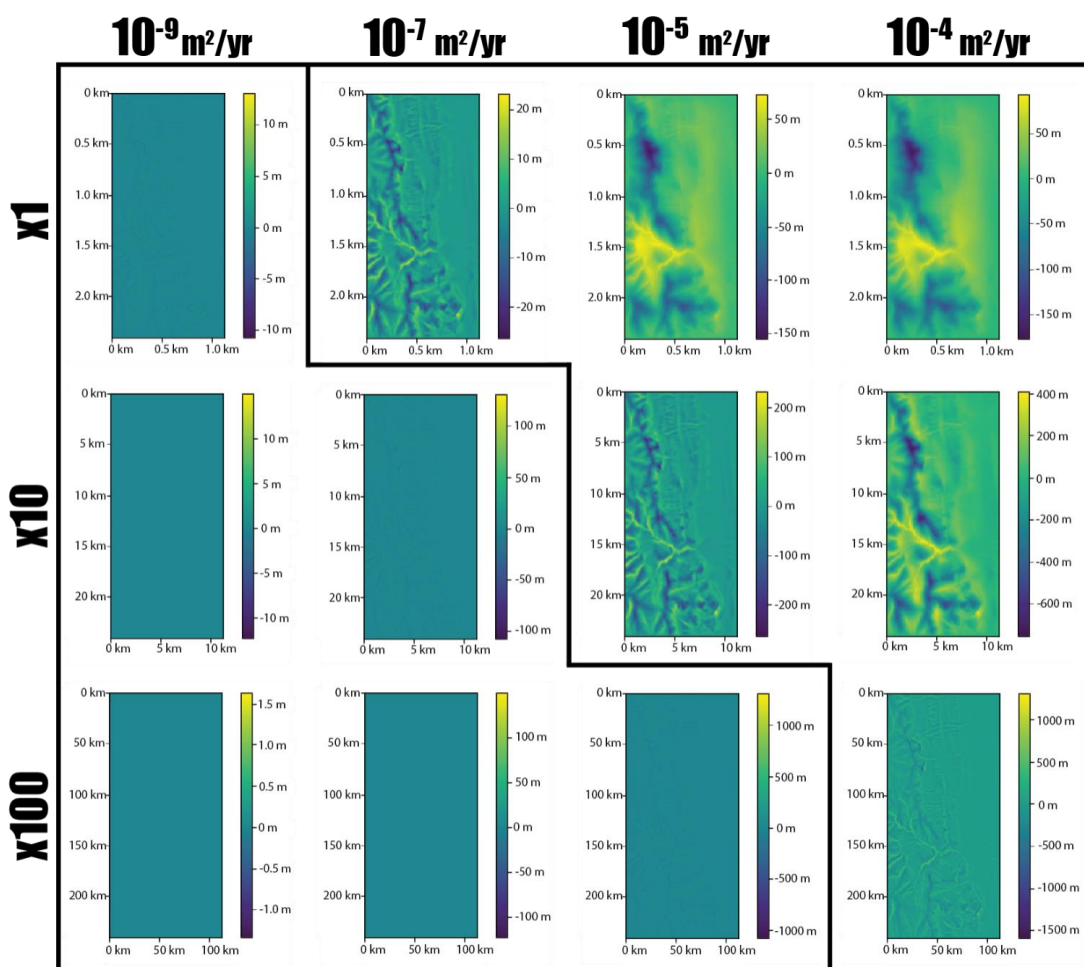


Figure 8. Shows difference maps made for each experiment by subtracting the initial DEM from the final DEM. The columns represent the different diffusivities used and the rows represent the different scales. The stair-step line separates the experiments that showed little difference (left) from those that noticeably eroded (right).

We chose two specific experiments to further examine using a topographic transect that captured each paleoshoreline in the initial DEM. These experiments (3 and 7, Table 2) were

performed using the same diffusivity value, $10^{-7} m^2 yr^{-1}$, but using two multipliers, $1\times$ and $10\times$. The $1\times$ experiment, being smaller scale, lost any identifiable paleoshoreline topographic features. Figure 9 shows a profile at $y = 1$ km of the initial topography, with breaks in slope from the three paleoshorelines denoted. Figure 9 shows the final transect topography from this experiment surrounded by the red box, and none of these features remain, with the important topographic breaks-in-slope being completely smoothed out. The opposite is true for the $10\times$ experiment, which retained its features. Figure 9 also shows the final transect topography for this experiment surrounded by the blue box. Though they slightly changed, those three topographic breaks in slope denoting the paleoshorelines still remained at the end of the simulated 3.5 Ga.

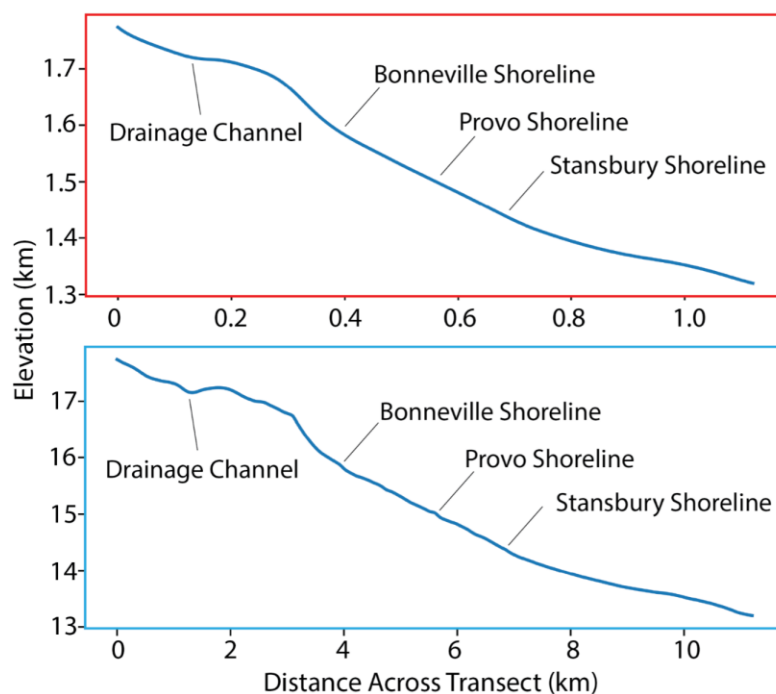


Figure 9. Shows final timestep transects for two experiments. The top one in the red box is from experiment 3 (Table 2) and the bottom one in the blue box is from experiment 7 (Table 2). The top profile shows complete erosion of any discernable paleoshoreline topographic features, with the landscape being completely smoothed out. The bottom profile retained its paleoshoreline topographic features.

Figure 10 shows distributions of initial and final slope for these two experiments. The histogram on top shows distributions for the 1× experiment with the red bars being the initial slopes and the black being the final. All the red bars denoting high slope values (around 60 - 80 degrees) were lost by the end of the experiment and an overall lowering in slope is seen by there being more values in the 20 – 30-degree range than initially present. The lower histogram shows initial slope values in blue and final in black for the 10× experiment. The distributions of these slopes are similar, with no noticeable loss in high slopes values or overall lowering of slope. This corresponds with this experiment showing retention of its subtle topographic paleoshoreline features.

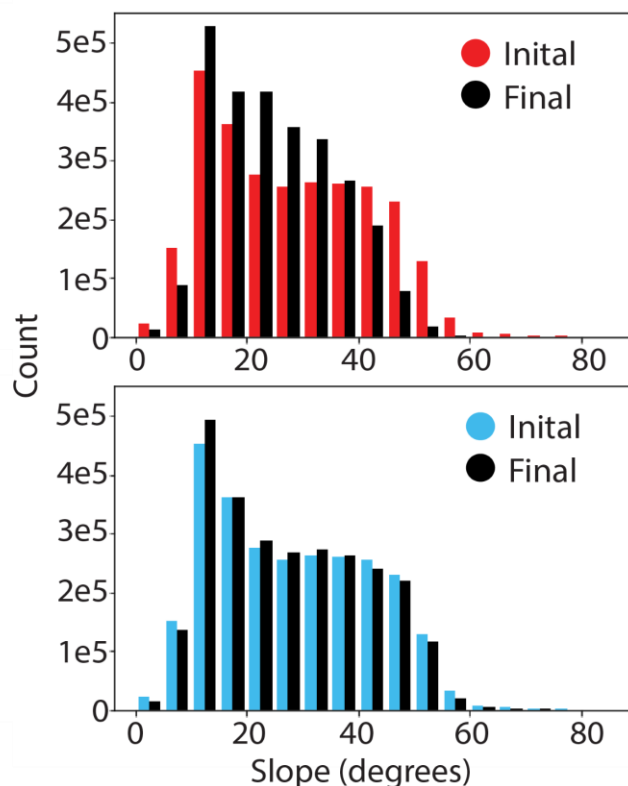


Figure 10. Shows slope distributions for experiments 3 and 7 (Table 2). The top histogram lost its high slope values and showed an overall decrease in the distribution whereas the bottom histogram's distribution remained largely the same.

Discussion

Despite there being variability paleoshoreline topographic features preservation across experimental parameter space, our results suggest that we should be skeptical of the previously interpreted Mars paleoshorelines. The only diffusivity value used that showed shoreline retention regardless of the scale modifier was the smallest Mars diffusivity, $10^{-9} m^2 yr^{-1}$. This value was estimated from impact crater erosion (Howard 2007; Golombek et al., 2014), located in hard Martian crust. However, Lake Bonneville paleoshorelines were carved into sedimentary rocks, which erode faster than hard crust. That $10^{-9} m^2 yr^{-1}$ value may not accurately represent their erosion since diffusivity may be lithology dependent (Martin, 2000; Richardson et al., 2019). Indeed, some stretches of proposed paleoshorelines on Mars expose stratigraphic layers, suggesting that have indeed undergone erosion and topographic modification since their formation (Sholes et al., 2019), consistent with our results.

Here, our model only accounted for erosion from topographic diffusion. However, diffusive hillslope processes may represent only a minor component of sedimentary rock erosion on Mars, with wind-driven sand abrasion performing most of the erosion (Cardenas et al., 2022). Prior work has suggested that aeolian abrasion may not behave diffusively (Cardenas et al., 2022), and so a potentially significant erosive process was not represented by the erosion in this model. Thus, the results from these twelve experiments are minimal-case scenarios for martian erosion, and any actual paleoshorelines formed 3.5 Ga on Mars may have undergone additional significant erosion via aeolian sand abrasion.

Ultimately, we suggest the most important result of our work is that the modern topography of Mars is at best an ambiguous representation of the ancient topography. There is evidence that some of the largest-scale topographic features, including the topographic dichotomy and large impact basins, have persisted for billions of years (Andrews-Hanna et al., 2008; Golombek et al., 2014). However, there is also evidence that sedimentary rocks, including those likely to host paleoshorelines, have been significantly reworked (Day et al., 2016; Sholes et al., 2019). In places, the erosion of sedimentary rock is estimated to have removed km of material over hundreds of km² (Cardenas and Lamb, 2022; Fassett and Head, 2008). We strongly suggest future studies of a martian ocean turn to the stratigraphic record which, rather than potentially being reworked by erosion, is revealed by it.

Conclusion

Here, we performed numerical experiments to test whether Earth-analog paleoshoreline topography might survive 3.5 Ga of diffusive erosion at Mars-like rates. Our experiments showed that paleoshoreline topography on Mars might have been susceptible to reworking, sometimes leaving key identifying features unrecognizable. Thus, true nature of many of these supposed Mars paleoshoreline is still up for debate. Instead of hoping to find fully preserved topography to infer ancient Mars oceans, we suggest turning to stratigraphic evidence instead, as erosion does not rework stratigraphy in the same manner as topography.

References

- Andrews-Hanna, J.C., Zuber, M.T., and Banerdt, B.W., 2008, The Borealis basin and the origin of the martian crustal dichotomy: *Nature*, v. 453, p. 1212-1215, doi: 10.1038/nature07011.
- Barnhart, K. R., Hutton, E. W. H., Tucker, G. E., Gasparini, N. M., Istanbuluoglu, E., Hopley, D. E. J., Lyons, N. J., Mouchene, M., Nudurupati, S. S., Adams, J. M., and Bandaragoda, C., 2020, Short communication: Landlab v2.0: A software package for Earth surface dynamics, *Earth Surf. Dynam.*, 8(2), p 379-397, doi:10.5194/esurf-8-379-2020.
- Benson, L.V., Lund, S.P., Smoot, J.P., Rhode, D.E., Spencer, R.J., Verosub, K.L., Louderback, L.A., Johnson, C.A., Rye, R.O., and Negrini, R.M., 2011, The rise and fall of Lake Bonneville between 45 and 10.5 ka: *Quaternary International*, v. 235, no. 1–2, p. 57–69, doi: 10.1016/j.quaint.2010.12.014.
- Cardenas, B.T., and Lamb, M.P., 2022, Paleogeographic reconstructions of an ocean margin on Mars based on deltaic sedimentology at Aeolis Dorsa: *Journal of Geophysical Research: Planets*, v. 127, doi: 10.1029/2022JE007390.
- Cardenas, B.T., Lamb, M.P., and Grotzinger, J.P., 2022, Martian landscapes of fluvial ridges carved from ancient sedimentary basin fill: *Nature Geoscience*, v. 15, p. 871-877, doi: 10.1038/s41561-022-01058-2.
- Carr, M., and Head, J., 2019, Mars: Formation and fate of a frozen Hesperian Ocean: *Icarus*, v. 319, p. 433–443, doi: 10.1016/j.icarus.2018.08.021.

- Carr, M. H., 2003, Oceans on Mars: An assessment of the observational evidence and possible fate. *Journal of Geophysical Research*, v. 108(E5), doi: 10.1029/2002je001963
- Carr, M.H., and Head, J.W., 2010, Geologic history of Mars: Earth and Planetary Science Letters, v. 294, no. 3–4, p. 185–203, doi: 10.1016/j.epsl.2009.06.042.
- DiBiase, R.A., Limaye, A.B., Scheingross, J.S., Fischer, W.W., and Lamb, M.P., 2013, Deltaic deposits at Aeolis Dorsa: Sedimentary evidence for a standing body of water on the Northern Plains of Mars: *Journal of Geophysical Research: Planets*, v. 118, no. 6, p. 1285–1302, doi: 10.1002/jgre.20100.
- Dickinson, W.R., 2001, Paleoshoreline record of relative holocene sea levels on Pacific Islands: *Earth-Science Reviews*, v. 55, no. 3–4, p. 191–234, doi: 10.1016/s0012-8252(01)00063-0.
- Diniega, S., Bramson, A.M., Buratti, B., Buhler, P., Burr, D.M., Chojnacki, M., Conway, S.J., Dundas, C.M., Hansen, C.J., McEwen, A.S., Lapôtre, M.G.A., Levy, J., Mc Keown, L., Piqueux, S., et al., 2021, Modern Mars' geomorphological activity, driven by wind, Frost, and gravity: *Geomorphology*, v. 380, p. 107627, doi: 10.1016/j.geomorph.2021.107627.
- Fassett, C., and Head, J.W., 2008, Layered mantling deposits in northeast Arabia Terra, Mars: Noachian-Hesperian sedimentation, erosion, and terrain inversion: *Journal of Geophysical Research: Planets*, v. 112, doi: 10.1029/2006JE002875.
- Golombek, M.P., Warner, N.H., Ganti, V., Lamb, M.P., Parker, T.J., Ferguson, R.L., and Sullivan, R., 2014, Small crater modification on Meridiani Planum and implications for

- erosion rates and climate change on Mars: *Journal of Geophysical Research: Planets*, v. 119, p. 2522-2547, doi: 10.1002/2014JE004658.
- Grotzinger, J.P., et al., 2015, Deposition, exhumation, and paleoclimate of an ancient lake deposit, Gale crater, Mars. *Science*, v. 350, doi: 10.1126/science.aac7575.
- Hare, J.L., Ferguson, J.F., Aiken, C.L., and Oldow, J.S., 2001, Quantitative characterization and elevation estimation of Lake Lahontan shoreline terraces from high-resolution digital elevation models: *Journal of Geophysical Research: Solid Earth*, v. 106, no. B11, p. 26761–26774, doi: 10.1029/2001jb000344.
- Head III, J.W., Kreslavsky, M., Hiesinger, H., Ivanov, M., Pratt, S., Seibert, N., Smith, D.E., and Zuber, M.T., 1998, Oceans in the past history of Mars: Tests for their presence using Mars Orbiter Laser Altimeter (MOLA) data: *Geophysical Research Letters*, v. 25, no. 24, p. 4401–4404, doi: 10.1029/1998gl900116.
- Hobley, D. E. J., Adams, J. M., Nudurupati, S. S., Hutton, E. W. H., Gasparini, N. M., Istanbuluoglu, E. and Tucker, G. E., 2017, Creative computing with Landlab: an openwa toolkit for building, coupling, and exploring two-dimensional numerical models of Earth-surface dynamics, *Earth Surface Dynamics*, 5(1), p 21-46, 10.5194/esurf-5-21-2017
- Howard, A.D., Moore, J.M., and Irwin, R.P., 2005, An intense terminal epoch of widespread fluvial activity on Mars: 1. Valley network incision and associated deposits. *Journal of Geophysical Research: Planets*, v. 110, doi: 10.1029/2005JE002459.

- Howard, A. D., 2007, Simulating the development of Martian highland landscapes through the interaction of impact cratering, fluvial erosion, and variable hydrologic forcing. *Geomorphology*, v, 91, no. 3-4, p. 332–363. doi: 10.1016/j.geomorph.2007.04.017
- Hughes, C.M., Cardenas, B.T., Goudge, T.A., and Mohrig, D., 2019, Deltaic deposits indicative of a paleo-coastline at Aeolis Dorsa, Mars: *Icarus*, v. 317, p. 442–453, doi: 10.1016/j.icarus.2018.08.009.
- Hutton, E., Barnhart, K., Hobley, D., Tucker, G., Nudurupati, S., Adams, J., Gasparini, N., Shobe, C., Strauch, R., Knuth, J., Mouchene, M., Lyons, N., Litwin, D., Glade, R., Giuseppicipolla95, Manaster, A., Abby, L., Thyng, K., and Rengers, F., 2020, landlab [Computer software]., doi: 10.5281/zenodo.595872
- Kite, E.S., and Mayer, D.P., 2017, Mars sedimentary rock erosion rates constrained using crater counts, with applications to organic-matter preservation and to the global dust cycle: *Icarus*, v. 286, p. 212–222, doi: 10.1016/j.icarus.2016.10.010.
- Malin, M.C., and Edgett, K.S., 1999, Oceans or seas in the Martian Northern Lowlands: High resolution imaging tests of proposed coastlines: *Geophysical Research Letters*, v. 26, no. 19, p. 3049–3052, doi: 10.1029/1999gl002342.
- Martin, Y., 2000, Modelling hillslope evolution: Linear and nonlinear transport relations: *Geomorphology*, v. 34, no. 1–2, p. 1–21, doi: 10.1016/s0169-555x(99)00127-0.
- Oviatt, C.G., 2015, Chronology of lake bonneville, 30,000 to 10,000 yr B.P.: *Quaternary Science Reviews*, v. 110, p. 166–171, doi: 10.1016/j.quascirev.2014.12.016.

- Parker, T.J., Gorsline, D.S., Saunders, R.S., Pieri, D.C., and Schneeberger, D.M., 1993, Coastal geomorphology of the Martian Northern Plains: *Journal of Geophysical Research: Planets*, v. 98, no. E6, p. 11061–11078, doi: 10.1029/93je00618.
- Parker, T.J., Stephen Saunders, R., and Schneeberger, D.M., 1989, Transitional morphology in west Deuteronilus Mensae, Mars: Implications for modification of the lowland/upland boundary: *Icarus*, v. 82, no. 1, p. 111–145, doi: 10.1016/0019-1035(89)90027-4.
- Perron, J.T., Mitrovica, J.X., Manga, M., Matsuyama, I., and Richards, M.A., 2007, Evidence for an ancient Martian ocean in the topography of deformed shorelines: *Nature*, v. 447, no. 7146, p. 840–843, doi: 10.1038/nature05873.
- Richardson, P.W., Perron, J.T., and Schurr, N.D., 2019, Influences of climate and life on Hillslope Sediment Transport: *Geology*, v. 47, no. 5, p. 423–426, doi: 10.1130/g45305.1.
- Sholes, S.F., Montgomery, D.R., and Catling, D.C., 2019, Quantitative high-resolution reexamination of a hypothesized ocean shoreline in Cydonia Mensae on Mars: *Journal of Geophysical Research: Planets*, v. 124, no. 2, p. 316–336, doi: 10.1029/2018je005837.
- Sholes, S.F., Dickeson, Z.I., Montgomery, D., and Catling, D., 2021, Where are Mars' hypothesized ocean shorelines? large lateral and topographic offsets between different versions of paleoshoreline maps., doi: 10.1002/essoar.10502868.2.
- Watters, T.R., McGovern, P.J., and Irwin III, R.P., 2007, Hemispheres apart: The crustal dichotomy on Mars: *Annual Review of Earth and Planetary Sciences*, v. 35, no. 1, p. 621–652, doi: 10.1146/annurev.earth.35.031306.140220.